Regulation of the Mdm2–p53 pathway by the ubiquitin E3 ligase MARCH7

Kailiang Zhao[1], Yang Yang[1], Guang Zhang[1], Chenfeng Wang[1], Decai Wang[1], Mian Wu[1,*] & Yide Mei[1,2,**]

Abstract

The tumor suppressor p53 plays a prominent role in the protection against cancer. The activity of p53 is mainly controlled by the ubiquitin E3 ligase Mdm2, which targets p53 for proteasomal degradation. However, the regulation of Mdm2 remains not well understood. Here, we show that MARCH7, a RING domain-containing ubiquitin E3 ligase, physically interacts with Mdm2 and is essential for maintaining the stability of Mdm2. MARCH7 catalyzes Lys^{63}-linked polyubiquitination of Mdm2, which impedes Mdm2 autoubiquitination and degradation, thereby leading to the stabilization of Mdm2. MARCH7 also promotes Mdm2-dependent polyubiquitination and degradation of p53. Furthermore, MARCH7 is able to regulate cell proliferation, DNA damage-induced apoptosis, and tumorigenesis via a p53-dependent mechanism. These findings uncover a novel mechanism for the regulation of Mdm2 and reveal MARCH7 as an important regulator of the Mdm2–p53 pathway.

Introduction

The tumor suppressor p53 plays a pivotal role in the protection against cancer [1–4]. In the development of more than half of human tumors, p53 is frequently inactivated by oncogenic mutations. Even in tumors with wild-type p53, the p53 pathway is often disrupted by either expression of oncoproteins or defective regulations upstream or downstream to p53 [1,5]. As a tumor suppressor, p53 activates anti-proliferative processes in response to a wide range of cellular stresses including DNA damage and oncogene activation. The extensively characterized responses invoked by p53 include cell cycle arrest, apoptosis, and senescence. Increasing evidence also suggests an important role of p53 in the regulation of cell metabolism, autophagy, and ferroptosis [6–10].

Due to the potent anti-proliferative effect of p53, it is not surprising that p53 function is strictly restrained in unstressed cells. p53 is primarily regulated at the level of stability. In unstressed cells, p53 levels are low due to its rapid ubiquitination and proteasomal degradation. The principle ubiquitin E3 ligase for p53 is Mdm2 [11–13], the importance of which is underscored by the findings that Mdm2 deficiency-caused early embryonic lethality in mice can be completely rescued by the concomitant deletion of p53 [14,15]. In addition to the trans-E3 ligase activity toward p53, Mdm2 also mediates its own degradation through a self-catalytic mechanism [16,17]. Under stress conditions, such as DNA damage, Mdm2 undergoes ataxia telangiectasia mutated (ATM)-mediated phosphorylation and subsequent degradation [18], thereby triggering p53 stabilization and activation. Once activated, p53 induces expression of a large number of genes that involve in various cellular processes such as cell cycle progression and apoptosis induction.

Mdm2 is considered an oncogene due to the ability of its product to inhibit p53 tumor suppressor function. In support of this, *Mdm2* gene amplification occurs in approximately 7% of all human cancers without concomitant p53 mutation [19–21], indicating that *Mdm2* gene amplification facilitates tumorigenesis by inhibiting p53-mediated tumor suppressive pathways. Moreover, Mdm2 is frequently overexpressed in childhood acute lymphoblastic leukemia by post-transcriptional mechanisms [22,23]. Intriguingly, over half of pediatric acute myelogenous leukemia patients examined exhibit the elevated Mdm2 protein levels, but without either *Mdm2* gene amplification or *p53* gene mutation[22], suggesting that the elevation of Mdm2 protein levels is likely due to post-transcriptional mechanisms and that Mdm2 protein overexpression is sufficient to abrogate p53 tumor suppressor function. Therefore, investigation of post-transcriptional regulation of Mdm2 is critical for the understanding of Mdm2 deregulation in human cancer.

To date, a number of ubiquitin E3 ligases and deubiquitinating enzymes have been implicated in the post-transcriptional regulation of Mdm2. For instance, PCAF, SCF$^{\beta\text{-TRCP}}$, XIAP, TRIM13, and NAT10 function as ubiquitin E3 ligases to promote the

1 CAS Key Laboratory of Innate Immunity and Chronic Disease, School of Life Sciences and Medical Center, University of Science & Technology of China, Hefei, Anhui, China
2 Hefei National Laboratory for Physical Sciences at Microscale, Hefei, Anhui, China
*Corresponding author. Tel: +86 0551 63606264; E-mail: wumian@ustc.edu.cn
**Corresponding author. Tel: +86 0551 63600921; E-mail: meiyide@ustc.edu.cn

ubiquitination and degradation of Mdm2 [24–28]. In contrast, several deubiquitinating enzymes, such as HAUSP, USP2a, and USP15, are able to stabilize Mdm2 by removing its polyubiquitin chains [29–32]. In addition, Mdm2 has also been shown to be stabilized by the structurally related Mdmx protein and several Mdmx spliced forms [33–37]. Although the deubiquitinating enzyme-mediated Mdm2 stabilization has been well recognized, it remains uncertain that whether Mdm2 stability is positively regulated by ubiquitin E3 ligase.

MARCH7 (membrane-associated RING-CH-type finger 7), also known as axotrophin, was originally identified in mouse embryonic stem cells with potential function in neural differentiation [38]. It was later found to be involved in the regulation of both neurological development and the immune system [39–41]. As a RING domain-containing ubiquitin E3 ligase, MARCH7 is able to promote the ubiquitination and degradation of the LIF receptor gp190 subunit [39]. The levels of MARCH7 itself are tightly controlled by both autoubiquitination and deubiquitination via the deubiquitinating enzymes USP7 and USP9X [42]. It has been recently shown that MARCH7 regulates NLRP3 inflammasome by binding to NLRP3 and promoting its ubiquitination and degradation [43]. Besides, MARCH7 is upregulated in ovarian cancer and promotes ovarian tumor growth [44], indicating the role of MARCH7 in the regulation of tumorigenesis.

In this study, we report MARCH7 as a novel interaction partner of Mdm2. Via the direct interaction, MARCH7 catalyzes Lys^{63}-linked polyubiquitination of Mdm2. This inhibits autoubiquitination and degradation of Mdm2 and thus increases its protein stability. Functionally, MARCH7 regulates cell proliferation, apoptosis, and tumorigenesis via the Mdm2–p53 axis. Collectively, these results reveal MARCH7 as a critical regulator of Mdm2 and define an important function of MARCH7 in the regulation of the Mdm2–p53 pathway.

Results

MARCH7 is an Mdm2-interacting protein

To better understand how the Mdm2–p53 axis is regulated, we employed an affinity purification method to identify novel Mdm2-interacting proteins. HCT116 cells were treated with formaldehyde to stabilize protein–protein interactions. Cell lysates were immunoprecipitated with either anti-Mdm2 antibody or an isotype-matched control IgG. The immunoprecipitated proteins were analyzed by mass spectrometry. MARCH7, a RING domain-containing ubiquitin E3 ligase, was identified in anti-Mdm2 immunoprecipitates (Fig 1A, Appendix Fig S1A, Dataset EV1).

To verify the interaction between MARCH7 and Mdm2, we expressed HA-MARCH7 alone or together with Flag-Mdm2 in HEK293T cells. An immunoprecipitation assay indicated a specific interaction of these two proteins (Fig 1B). A reciprocal immunoprecipitation experiment using lysates from HEK293T cells expressing Flag-MARCH7 and HA-Mdm2 also confirmed the MARCH7–Mdm2 interaction (Fig 1C). Using a co-immunoprecipitation assay with anti-Mdm2 antibody, the interaction between endogenous MARCH7 and Mdm2 was readily detected (Fig 1D). The ubiquitin E3 ligase activity of MARCH7 appears to be dispensable for its interaction

with Mdm2, because MARCH7 W589A/I556A, a E2 binding-defective mutant lacking of the ubiquitin E3 ligase activity [42], was still able to interact with Mdm2 (Fig 1E). Furthermore, an *in vitro* binding assay with purified MARCH7 and Mdm2 proteins showed that MARCH7 directly associated with Mdm2 (Fig 1F). The immunofluorescence assay showed that ectopically expressed MARCH7 and Mdm2 were co-localized in the nucleus, suggesting that the MARCH7–Mdm2 interaction occurs in the nucleus (Appendix Fig S1B). Together, these results demonstrate that MARCH7 is a novel binding partner for Mdm2.

To identify the regions of Mdm2 that are responsible for its interaction with MARCH7, we generated a panel of Mdm2 deletion mutants (Fig 2A). Mdm2 (aa 1–199) exhibited no interaction with MARCH7, while both Mdm2 (aa 100–299) and Mdm2 (aa 300–491) strongly associated with MARCH7 (Fig 2B), suggesting that the central acidic region and C-terminal RING domain likely mediate the interaction of Mdm2 with MARCH7. To delineate the Mdm2-binding domains in MARCH7, we also generated a panel of MARCH7 deletion mutants (Fig 2C). N-terminal region (aa 1–542) and C-terminal regions (aa 617–704 and aa 543–704) of MARCH7 strongly bound to Mdm2, while the RING domain (aa 543–616) exhibited no binding (Fig 2D). These data suggest that both N- and C-terminal regions (aa 1–542 and aa 617–704) of MARCH7 mediate the interaction with Mdm2.

MARCH7 increases the stability of Mdm2

Given the interaction of MARCH7 with Mdm2, we sought to investigate whether MARCH7 regulates Mdm2. Knockdown of MARCH7 using short hairpin (sh) RNA resulted in a substantial reduction of the steady-state levels of Mdm2 in p53-deficient ($p53^{-/-}$) HCT116 cells (Fig 3A, Appendix Fig S2A). When MARCH7 was co-expressed with Mdm2 in HEK293T cells, the levels of Mdm2 were increased by MARCH7 in a dose-dependent manner (Fig 3B, lanes 1–3, Appendix Fig S2B). However, in the presence of the proteasome inhibitor MG132, MARCH7 no longer enhanced the levels of Mdm2 (Fig 3B, lanes 4–6, Appendix Fig S2B), indicating that MARCH7 prevents proteasomal degradation of Mdm2. Unlike wild-type MARCH7, the ubiquitin E3 ligase-inactive mutant (W589A/I556A) of MARCH7 failed to enhance Mdm2 levels (Fig 3C, Appendix Fig S2C), although this mutant retained the Mdm2-binding ability (Fig 1E and F), suggesting that the ubiquitin E3 ligase activity of MARCH7 is essential for regulating Mdm2. In addition, unlike wild-type MARCH7, an Mdm2 binding-defective mutant of MARCH7 (aa 543–616) failed to increase Mdm2 levels (Fig 2D, Appendix Fig S2D), indicating that the interaction with Mdm2 is also critical for MARCH7 to regulate Mdm2 levels.

It has been well characterized that Mdm2 is subjected to autoubiquitination and rapid degradation [16,17]. We therefore asked whether MARCH7 is still able to regulate Mdm2 levels when Mdm2 autoubiquitination cannot occur. The ubiquitin E3 ligase-inactive mutant (C464A) of Mdm2 [17], devoid of autoubiquitination, was used. When this Mdm2 mutant was co-expressed with MARCH7 in HEK293T cells, its levels were not regulated by MARCH7 (Fig 3D, Appendix Fig S2E). The failure of MARCH7 to regulate Mdm2 C464A levels is not due to the loss of their interaction (Fig 3E). Together, these data indicate that MARCH7 enhances
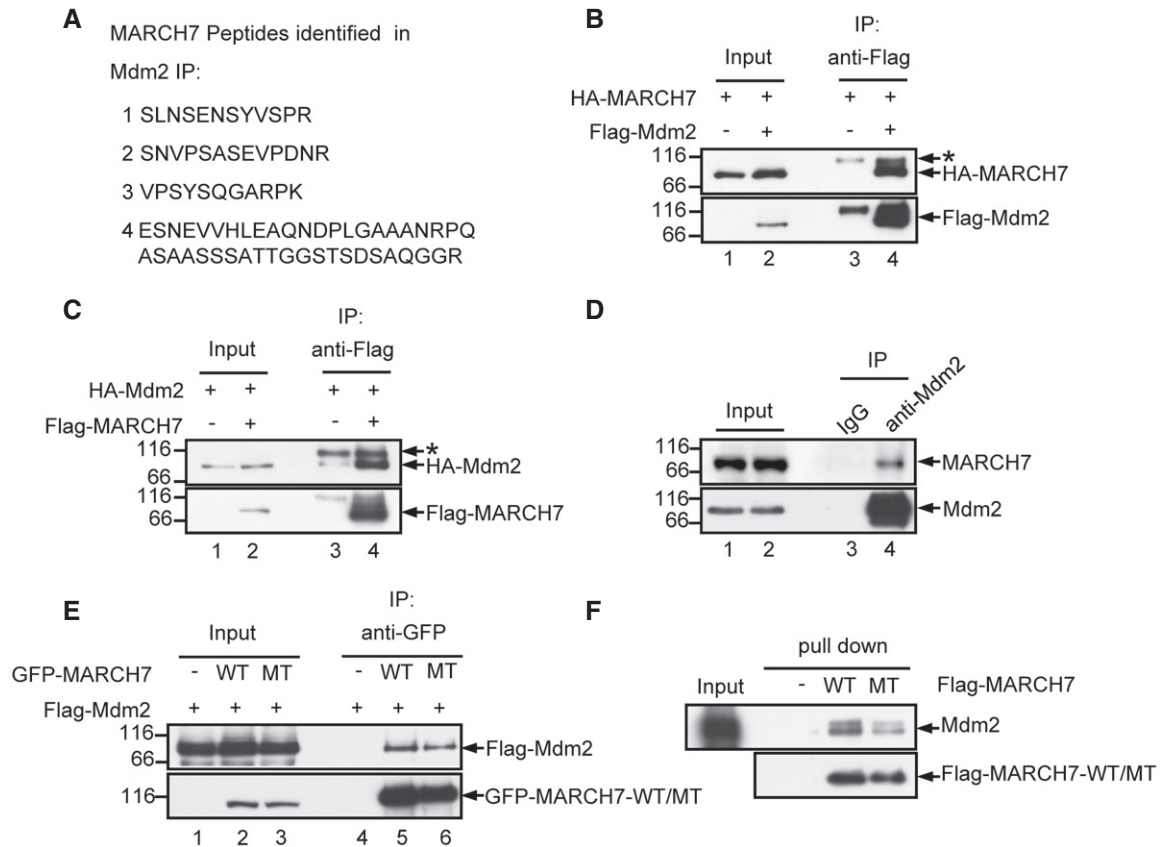
Figure 1. MARCH7 interacts with Mdm2 both *in vitro* and *in vivo*.

A   Lysates from HCT116 cells were immunoprecipitated with anti-Mdm2 antibody. The immunoprecipitated proteins were characterized by mass spectrometry analysis. MARCH7 was identified in Mdm2 precipitates, and the MARCH7 peptide sequences obtained by MS are shown.

B   HEK293T cells were transfected with either HA-MARCH7 alone or together with Flag-Mdm2. Twenty-four hours after transfection, cell lysates were subjected to immunoprecipitation with anti-Flag antibody. The immunoprecipitates and input were analyzed by Western blotting. Molecular weight standards (in kDa) are shown on the left. * indicates a non-specific band.

C   HEK293T cells were transfected with HA-Mdm2 alone or together with Flag-MARCH7. Twenty-four hours later, cell lysates were immunoprecipitated with anti-Flag antibody, followed by Western blot analysis. * indicates a non-specific band.

D   Lysates from HCT116 cells were immunoprecipitated separately with anti-Mdm2 antibody or an isotype-matched control IgG. The immunoprecipitates and input were analyzed by Western blotting.

E   HEK293T cells were transfected with Flag-Mdm2 alone, Flag-Mdm2 plus GFP-MARCH7-WT (wild-type), or Flag-Mdm2 plus GFP-MARCH7-MT (W589A/I556A). Cell lysates were subjected to immunoprecipitation with anti-GFP antibody, followed by Western blot analysis.

F   Purified Flag-MARCH7-WT (wild-type) or Flag-MARCH7-MT (W589A/I556A) immobilized on beads was incubated with purified Mdm2. Input and beads-bound proteins were analyzed by Western blotting with anti-Mdm2 antibody.

Mdm2 levels by inhibiting autoubiquitination and degradation of Mdm2.

To determine the mechanism by which MARCH7 enhances Mdm2 levels, we evaluated the effect of MARCH7 on the stability of Mdm2 protein. HA-Mdm2 was co-expressed in HEK293T cells with or without Flag-MARCH7. The ectopic expression of MARCH7 prolonged the half-life of Mdm2 (Fig 3F, Appendix Fig S2F). Conversely, when MARCH7 was knocked down in U2OS cells, the half-life of Mdm2 was shortened (Fig 3G, Appendix Fig S2G), indicating an important role of MARCH7 in regulating Mdm2 stability. Consistent with the previous findings [42], MARCH7 itself is a labile protein with half-life shorter than 30 min (Fig 3G). Of note, knockdown of MARCH7 led to the increased stability of p53 in U2OS cells (Fig 3G, Appendix Fig S2H), implying that MARCH7 may regulate the Mdm2–p53 axis.

MARCH7 promotes Mdm2-dependent polyubiquitination and degradation of p53

To determine the effect of MARCH7 on the Mdm2–p53 axis, we knocked down MARCH7 in p53 wild-type U2OS and HCT116 cells. In these cells, MARCH7 knockdown resulted in the reduction of Mdm2 levels, which was accompanied with the enhancement of p53 levels (Fig 4A, Appendix Fig S3A). The accumulated p53 protein was functional as shown by the increased expression of the p53 target gene *p21* (Fig 4A). Similar results were also obtained in human primary fibroblasts IMR90 (Fig 4B, Appendix Fig S3B). To rule out the potential off-target effect of sh-MARCH7, we used two additional MARCH7 targeting shRNAs (sh-MARCH7-#2 and sh-MARCH7-#3). Knockdown of MARCH7 by either sh-MARCH7-#2 or sh-MARCH7-#3 consistently led to a decrease in Mdm2 levels and
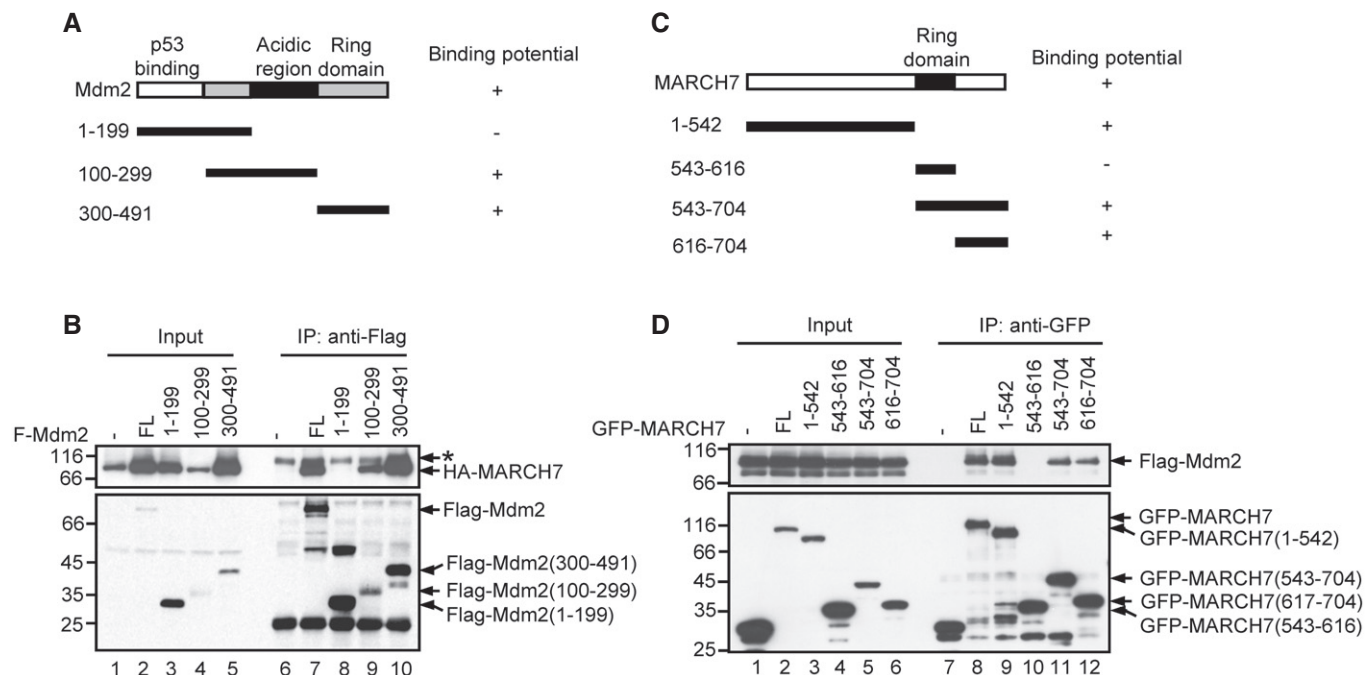
Figure 2. Mapping of interaction regions between MARCH7 and Mdm2.

A Schematic representation of wild-type Mdm2 and the indicated deletion mutants.

B HEK293T cells were transfected with HA-MARCH7 alone or together with the indicated Flag-Mdm2 constructs. Cell lysates were subjected to immunoprecipitation with anti-Flag antibody, followed by Western blot analysis. * indicates a non-specific band.

C Schematic representation of wild-type MARCH7 and its deletion mutants.

D HEK293T cells were transfected with Flag-Mdm2 alone or together with the indicated GFP-MARCH7 constructs. Cell lysates were subjected to immunoprecipitation with anti-GFP antibody, followed by Western blot analysis.

an increase in p53 levels (Fig 4C, Appendix Fig S3C), indicating the specific regulatory effect of MARCH7 on the levels of Mdm2 and p53.

We next determined whether the effect of MARCH7 on p53 levels is mediated by Mdm2. The Mdm2–p53 interaction inhibitor Nutlin-3 was utilized. Knockdown of MARCH7 consistently led to a great increase in the levels of p53 in HCT116 cells (Fig 4D, lanes 1 and 2, Appendix Fig S3D). However, when these cells were treated with Nutlin-3, MARCH7 knockdown no longer showed any regulatory effect on p53 levels (Fig 4D, lanes 3 and 4, Appendix Fig S3D). To further confirm that MARCH7 promotes Mdm2-dependent p53 degradation, we evaluated the effect of MARCH7 on the polyubiquitination of endogenous p53. The results showed that knockdown of MARCH7 greatly decreased, whereas ectopic expression of MARCH7 markedly increased the polyubiquitination of p53 (Fig 4E and F). More importantly, when the Mdm2–p53 interaction was disrupted by Nutlin-3, MARCH7 failed to enhance the polyubiquitination of p53 (Fig 4F). Together, these data imply that the effect of MARCH7 on p53 levels is mediated by Mdm2.

To extend these analyses, we expressed p53 together with Mdm2 or MARCH7 or both in mouse embryonic fibroblast (MEF) cells deficient in both p53 and Mdm2. When MARCH7 was co-expressed with p53 in these cells, MARCH7 had minimal effect on p53 in the absence of Mdm2 (Fig 4G, lanes 1–3, Appendix Fig S3E). However, with the additional expression of Mdm2, MARCH7 enhanced p53 degradation (Fig 4G, lanes 4–6, Appendix Fig S3E). MARCH7 was also shown to enhance Mdm2-mediated p53 polyubiquitination in a dose-dependent manner (Fig 4H, lanes 4–6). In these experiments, MARCH7 did not affect p53 polyubiquitination in the absence of Mdm2 (Fig 4H, lanes 1–3). Taken together, these data strongly suggest that MARCH7 promotes p53 polyubiquitination and degradation in an Mdm2-dependent manner.

Given the inhibitory effect of MARCH7 on p53 levels, we examined whether MARCH7 regulates p53 target gene expression. As was expected, knockdown of MARCH7 greatly elevated the mRNA levels of p53 target genes such as *p21, DRAM, TIGAR, Sestrin, Puma,* and *Noxa,* while p53 mRNA levels remained relatively unaffected (Fig 4I). To determine the effect of MARCH7 on p53 transcriptional activity, we used two p53-responsive reporter plasmids, pGL3-p21-luc and pGL3-Noxa-luc, in which the luciferase gene is controlled by the p21 and Noxa promoters, respectively. When either of these two reporter plasmids was introduced in U2OS cells, knockdown of MARCH7 potently activated luciferase expression (Fig 4J). We also evaluated the effect of MARCH7 on p53 transcriptional activity in $Mdm2^{-/-}p53^{-/-}$ MEF cells. In accordance with the findings that MARCH7 enhanced Mdm2-dependent polyubiquitination and degradation of p53 (Fig 4G and H), MARCH7 decreased p53 transcriptional activity in the presence, but not in the absence of Mdm2 (Appendix Fig S3F). These results indicate that MARCH7 indeed regulates p53 transcriptional activity.
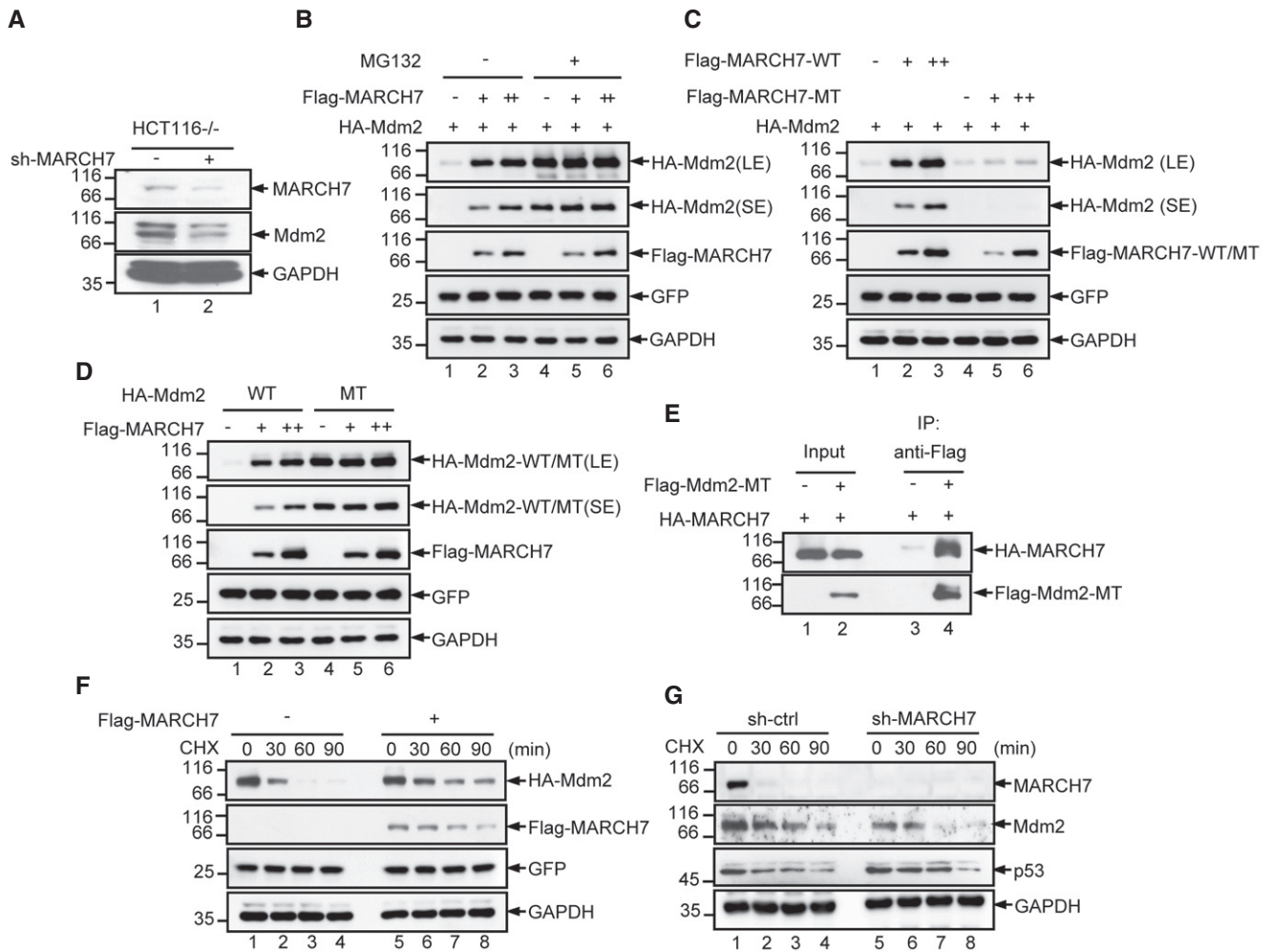
Figure 3. MARCH7 regulates the stability of Mdm2.

A HCT116 $p53^{-/-}$ cells were infected with lentiviruses expressing either control shRNA or MARCH7 shRNA. Forty-eight hours after infection, cell lysates were subjected to Western blot analysis with antibodies against the indicated proteins. The data are representative of at least three biological replicates. The band intensities were quantified by using ImageJ software. The ratio of Mdm2 to GAPDH is presented in Appendix Fig S2A.

B HEK293T cells were transfected with HA-Mdm2 alone or together with increasing amounts of Flag-MARCH7. Twenty-four hours later, cells were treated with or without 20 μM MG132 for an additional 6 h. Cell lysates were then analyzed by Western blotting. Levels of GFP and GAPDH were used as controls for transfection efficiency and sample loading, respectively. The data are representative of at least three biological replicates. The ratio of Mdm2 to GFP is presented in Appendix Fig S2B. LE and SE indicate long-time exposure and short-time exposure, respectively.

C HEK293T cells were transfected with HA-Mdm2 alone or together with increasing amounts of the indicated Flag-MARCH7 constructs. Cell lysates were analyzed by Western blotting. The data are representative of at least three biological replicates. The ratio of Mdm2 to GFP is presented in Appendix Fig S2C. LE and SE indicate long-time exposure and short-time exposure, respectively.

D HEK293T cells were transfected with HA-Mdm2 (WT) alone, HA-Mdm2 C464A mutant (MT) alone, or together with increasing amounts of Flag-MARCH7 as indicated. Twenty-four hours later, cell lysates were analyzed by Western blotting. The data are representative of at least three biological replicates. The ratio of Mdm2 to GFP is presented in Appendix Fig S2E. LE and SE indicate long-time exposure and short-time exposure, respectively.

E HEK293T cells were transfected with HA-MARCH7 alone, or together with Flag-Mdm2 C464A mutant (MT). Cell lysates were subjected to immunoprecipitation with anti-Flag antibody, followed by Western blot analysis.

F HEK293T cells were transfected with HA-Mdm2 alone, or together with Flag-MARCH7. Twenty-four hours later, cells were treated with 20 μg/ml cycloheximide (CHX) for the indicated periods of time. Cell lysates were then analyzed by Western blotting with the indicated antibodies. The data are representative of three biological replicates. The band intensities were quantified by using ImageJ software. The ratio of Mdm2 to GFP is presented in Appendix Fig S2F.

G HCT116 cells were infected with lentiviruses expressing either control shRNA or MARCH7 shRNA. Forty-eight hours later, cells were treated with 20 μg/ml cycloheximide (CHX) for the indicated periods of time. Cell lysates were then analyzed by Western blotting. The data are representative of three biological replicates. The ratios of Mdm2 to GAPDH and p53 to GAPDH are presented in Appendix Fig S2G and H, respectively.

MARCH7 catalyzes Lys^{63}-linked polyubiquitination of Mdm2

We next sought to investigate how Mdm2 is stabilized by MARCH7. The previously reported ubiquitin E3 ligase function of MARCH7 prompted us to ask whether MARCH7 could promote the polyubiquitination of Mdm2. We first performed an *in vivo* ubiquitination assay. We found that MARCH7 had no obvious effect on the polyubiquitination of wild-type Mdm2 (Fig 5A, lanes 1–3). Intriguingly,
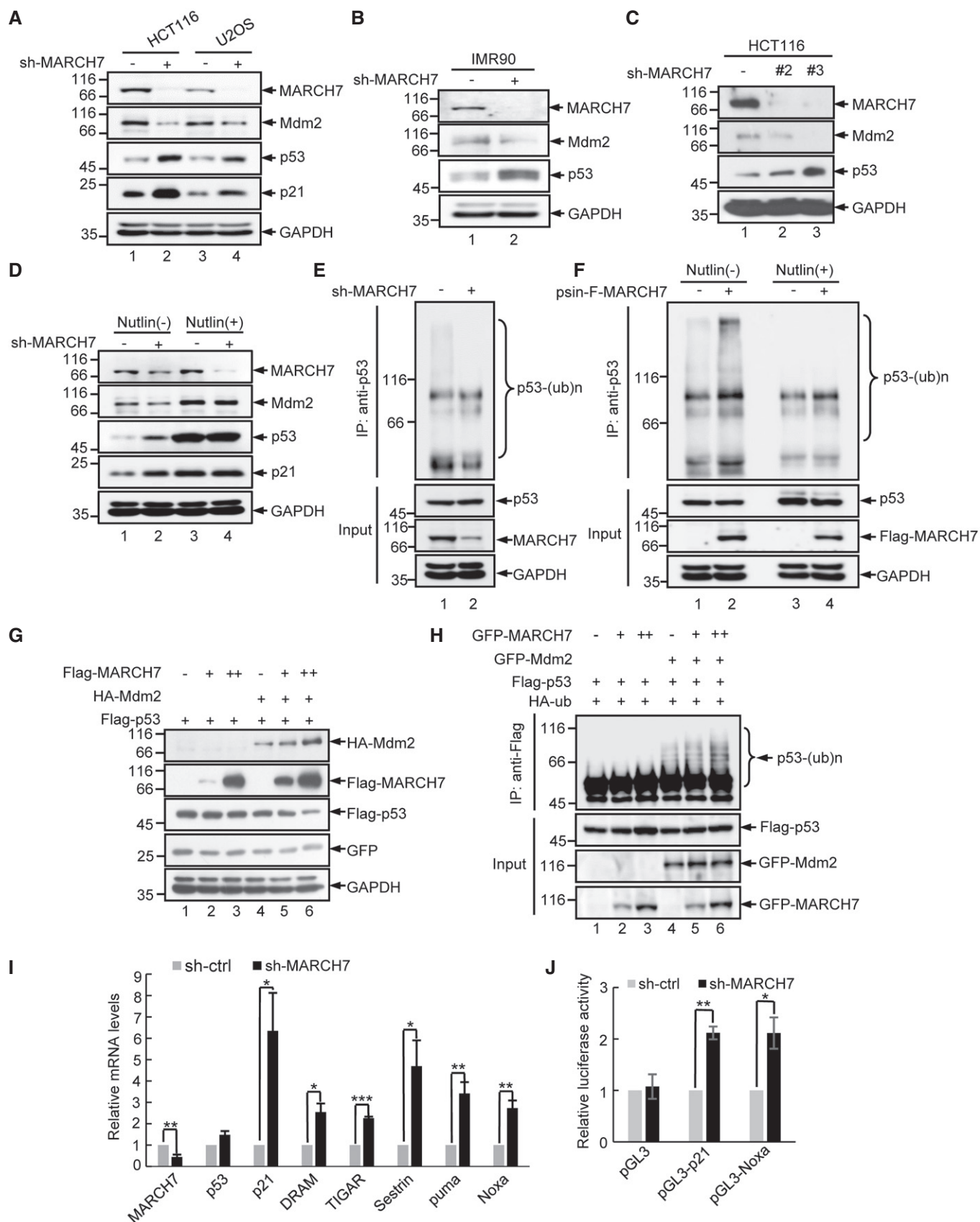
Figure 4.

◀

Figure 4.   MARCH7 regulates the Mdm2–p53 axis.

A   HCT116 and U2OS cells were infected with lentiviruses expressing either control shRNA or MARCH7 shRNA. Forty-eight hours later, cell lysates were subjected to Western blot analysis with the indicated antibodies. The data are representative of at least three biological replicates. The band intensities were quantified by using ImageJ software. The ratios of Mdm2 to GAPDH and p53 to GAPDH are presented in Appendix Fig S3A.

B   IMR90 cells were infected with lentiviruses expressing either control shRNA or MARCH7 shRNA. Forty-eight hours later, cell lysates were subjected to Western blot analysis with the indicated antibodies. The data are representative of at least three biological replicates. The ratios of Mdm2 to GAPDH and p53 to GAPDH are presented in Appendix Fig S3B.

C   HCT116 cells were infected with lentiviruses expressing control shRNA or two MARCH7 shRNAs (sh-MARCH7-#2 and sh-MARCH7-#3) as indicated. Forty-eight hours after infection, cell lysates were analyzed by Western blotting. The data are representative of three biological replicates. The ratios of Mdm2 to GAPDH and p53 to GAPDH are presented in Appendix Fig S3C.

D   HCT116 cells were infected with lentiviruses expressing either control shRNA or MARCH7 shRNA. Forty-eight hours later, cells were treated with or without 10 μM Nutlin-3 for an additional 24 h, followed by Western blot analysis. The data are representative of three biological replicates. The ratios of Mdm2 to GAPDH and p53 to GAPDH are presented in Appendix Fig S3D.

E   HCT116 cells were infected with lentiviruses expressing either control shRNA or MARCH7 shRNA. Forty-eight hours later, cells were treated with MG132 for an additional 6 h. Cell lysates were immunoprecipitated with anti-p53 antibody, followed by Western blot analysis with anti-ubiquitin antibody. Treatment with MG132 stabilized and eventually equalized the levels of p53 in the inputs.

F   HCT116 cells were infected with lentiviruses expressing control or MARCH7 proteins. Cells were then treated with or without 10 μM Nutlin-3 for 24 h before they were treated with MG132 for an additional 6 h. Cell lysates were immunoprecipitated with anti-p53 antibody, followed by Western blot analysis with anti-ubiquitin antibody. Treatment with MG132 stabilized and eventually equalized the levels of p53 in the inputs.

G $Mdm2^{-/-}p53^{-/-}$ MEF cells were transfected with Flag-p53, HA-Mdm2, and increasing amounts of Flag-MARCH7 as indicated. Twenty-four hours after transfection, cell lysates were subjected to Western blot analysis. The data are representative of three biological replicates. The ratio of p53 to GFP is presented in Appendix Fig S3E.

H $Mdm2^{-/-}p53^{-/-}$ MEF cells were transfected with Flag-p53, GFP-Mdm2, HA-Ub, and increasing amounts of GFP-MARCH7 as indicated. Twenty-four hours after transfection, cells were treated with MG132 for an additional 6 h. Cell lysates were immunoprecipitated with anti-Flag antibody, followed by Western blot analysis.

I   U2OS cells were infected with lentiviruses expressing either control shRNA or MARCH7 shRNA. Forty-eight hours later, total RNA was subjected to real-time RT–PCR analysis. Statistical analysis was carried out using Microsoft Excel software and GraphPad Prism to assess differences between experimental groups. Statistical significance was analyzed by Student's t-test and expressed as a P-value. The shown data are mean ± SD of three independent experiments. *, **, and *** indicate $P < 0.05$, $P < 0.01$, and $P < 0.001$, respectively.

J   U2OS cells expressing either control shRNA or MARCH7 shRNA were transfected with pGL3 control vector, pGL3-p21-luc, or pGL3-Noxa-luc as indicated. Twenty-four hours after transfection, the reporter activity was measured and plotted after normalizing with respect to Renilla luciferase activity. Statistical analysis was carried out using Microsoft Excel software and GraphPad Prism to assess differences between experimental groups. Statistical significance was analyzed by Student's t-test and expressed as a P-value. The shown data are mean ± SD of three independent experiments. * and ** indicate $P < 0.05$ and $P < 0.01$, respectively.

when the autoubiquitination of Mdm2 was blocked by its C464A mutation, MARCH7 was shown to promote this Mdm2 mutant polyubiquitination (Fig 5A, lanes 4–6), implying that the effect of MARCH7 on wild-type Mdm2 polyubiquitination may be masked by Mdm2 autoubiquitination. The MARCH7-promoted Mdm2 C464A polyubiquitination also occurred under denaturing conditions (Appendix Fig S4A). Compared with wild-type MARCH7, neither the ubiquitin E3 ligase-inactive mutant of MARCH7 (W589A/I556A) nor the Mdm2 binding-defective mutant of MARCH7 (aa 543–616) showed any effect on the polyubiquitination of Mdm2 C464A (Fig 5B, Appendix Fig S4B). To further determine whether MARCH7 acts as a ubiquitin E3 ligase for Mdm2, an *in vitro* ubiquitination

assay was performed with purified recombinant proteins. Consistent with the above findings (Fig 5A and B, Appendix Fig S4A), MARCH7 indeed enhanced the polyubiquitination of Mdm2 C464A (Fig 5C, lanes 5–8), but not wild-type Mdm2 (Fig 5C, lanes 1–4) *in vitro*.

Polyubiquitination usually occurs at Lys^{48} and Lys^{63} of ubiquitin. It has been well recognized that while Lys^{48}-linked polyubiquitination serves as a universal recognition signal that targets proteins for proteasomal degradation, Lys^{63}-linked polyubiquitination acts primarily as regulatory rather than proteolytic signal [45,46]. To determine the type of Mdm2 C464A polyubiquitination chain induced by MARCH7, we performed the ubiquitination assay with

Figure 5.   MARCH7 promotes Lys^{63}-linked polyubiquitination of Mdm2.

A   HEK293T cells were co-transfected with the indicated plasmids. Twenty-four hours after transfection, cells were treated with MG132 for an additional 6 h. Cell lysates were immunoprecipitated with anti-Flag antibody, followed by Western blot analysis.

B   HEK293T cells were co-transfected with the indicated plasmids. Twenty-four hours later, cells were treated with MG132 for an additional 6 h. Cell lysates were then immunoprecipitated with anti-Flag antibody, followed by Western blot analysis.

C   Recombinant wild-type Mdm2 (WT) or Mdm2 C464A mutant (MT) proteins were incubated with E1 (50 nM), E2 (UbcH5a, 500 nM), Flag-ubiquitin (200 μM), and either Flag-MARCH7 (WT) or Flag-MARCH7 W589A/I556A (MT) in 20 μl of *in vitro* ubiquitination reaction buffer. The reaction mixtures were analyzed by Western blotting with anti-Mdm2 antibody.

D   HEK293T cells were transfected with Flag-Mdm2 C464A (MT), GFP-MARCH7, HA-UbK48R, and HA-UbK63R in the indicated combinations. Twenty-four hours later, cells were treated with MG132 for an additional 6 h. Cell lysates were then subjected to immunoprecipitation, followed by Western blot analysis.

E   HEK293T cells were co-transfected with the indicated plasmids. Twenty-four hours after transfection, cells were treated with MG132 for an additional 6 h. Cell lysates were then immunoprecipitated with anti-Flag antibody, followed by Western blot analysis.

F   HCT116 cells were infected with lentiviruses expressing either control or Flag-MARCH7 proteins. Forty-eight hours later, cells were treated with MG132 for an additional 6 h. Cell lysates were then immunoprecipitated with anti-Mdm2 antibody, followed by Western blot analysis with anti-ubiquitin (K63-linkage specific) antibody.

▶

ubiquitin mutants UbK48R (Lys48 replaced by Arg), UbK63R (Lys63 replaced by Arg), Ub48K (lack all lysine residues except Lys48), and Ub63K (lack all lysine residues except Lys63). The results showed that MARCH7 greatly enhanced the polyubiquitination of Mdm2 C464A in the presence of UbK48R but not UbK63R (Fig 5D). In addition, MARCH7 induced polyubiquitination of Mdm2 C464A in the
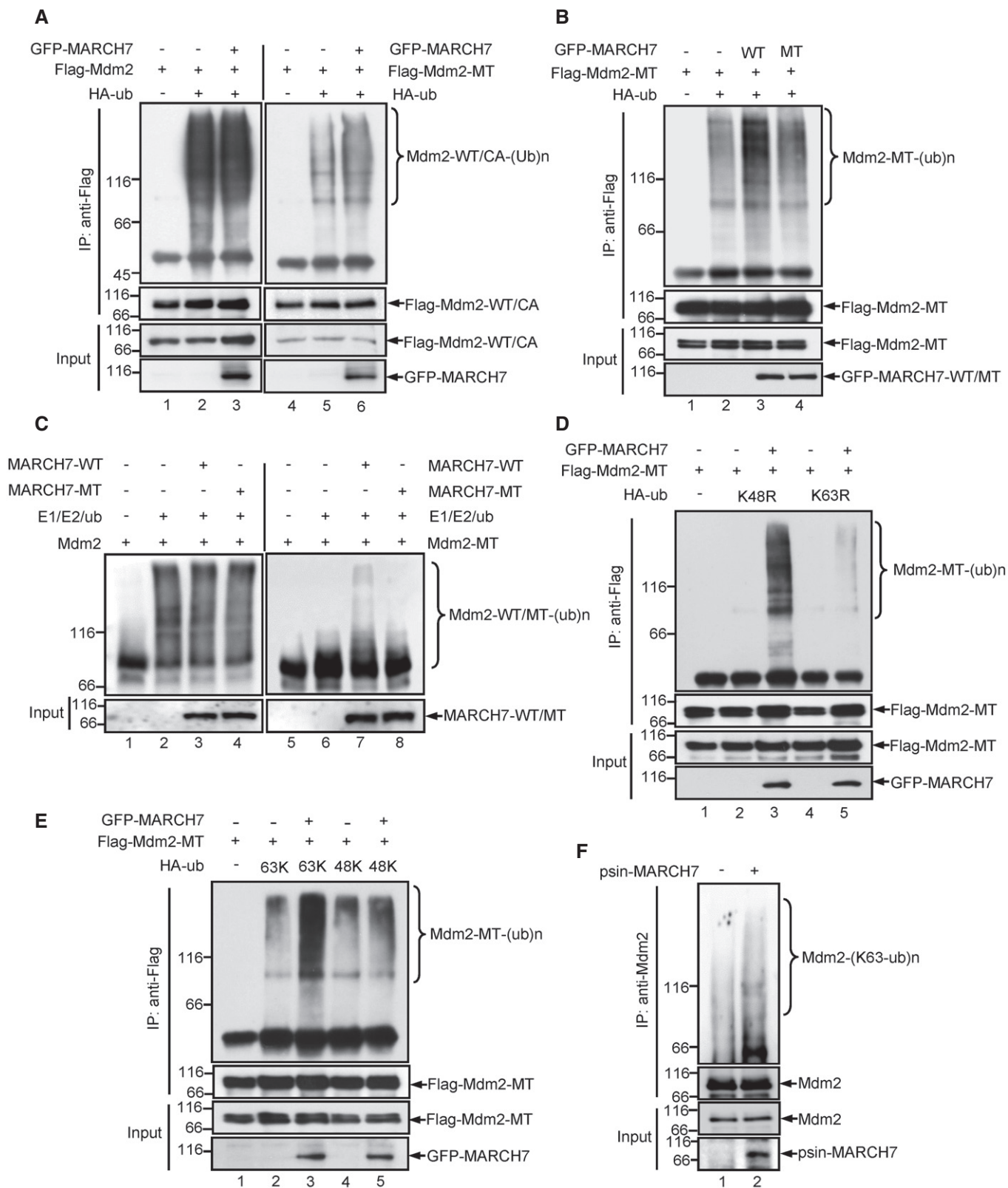

Figure 5.

presence of Ub63K but not Ub48K (Fig 5E). These data suggest that MARCH7 promotes Lys^{63}-linked polyubiquitination of Mdm2 C464A. To further determine whether MARCH7 promotes Lys^{63}-linked polyubiquitination of endogenous Mdm2, we performed an *in vivo* ubiquitination experiment in HCT116 cells stably expressing either control or MARCH7 proteins. The results showed that ectopic expression of MARCH7 was indeed able to increase Lys^{63}-linked polyubiquitination of endogenous Mdm2 (Fig 5F). Together with the findings that MARCH7 enhanced the levels of wild-type Mdm2 but not its ubiquitin E3 ligase-inactive C464A mutant (Fig 3D), these data imply that MARCH7 promotes Lys^{63}-linked polyubiquitination of Mdm2, which impedes Mdm2 autoubiquitination and degradation, thereby leading to the stabilization of Mdm2.

MARCH7 regulates cell proliferation, apoptosis, and tumorigenesis in a p53-dependent manner

To determine the functional consequence of MARCH7-mediated regulation of the Mdm2–p53 axis, we evaluated the effect of MARCH7 on cell proliferation, p53-mediated apoptosis, and tumorigenesis. MARCH7 and p53 were knocked down individually or combined in U2OS cells. Knockdown of MARCH7 effectively inhibited the proliferation of U2OS cells, which could be partially restored by the simultaneous knockdown of p53 (Fig 6A, Appendix Fig S5A). Similar results were also obtained in HCT116 cells (Appendix Fig S5B and C). To further confirm the effect of MARCH7 on cell proliferation is mediated by p53, the paired HCT116 cell lines ($p53^{+/+}$ and $p53^{-/-}$) were used. Knockdown of MARCH7 markedly inhibited the proliferation of HCT116 $p53^{+/+}$ cells, but not HCT116 $p53^{-/-}$ cells (Fig 6B, Appendix Fig S5D). To determine whether the effect of MARCH7 on cell proliferation also occurs in normal cells, the normal mouse embryo fibroblast (MEF) cells were used. Knockdown of MARCH7 greatly inhibited the proliferation of MEF cells, however, which could be reversed by the simultaneous knockdown of p53 (Fig 6C, Appendix Fig S5E).

These data suggest that MARCH7 regulates cell proliferation in a p53-dependent manner.

Given the effect of MARCH7 on p53 levels under non-stressed condition, we next sought to examine whether MARCH7 regulates the p53 response to DNA damage. U2OS cells stably expressing either MARCH7 shRNA or ectopic MARCH7 protein were treated with the DNA-damaging agent doxorubicin. Knockdown of MARCH7 resulted in an earlier and stronger p53 accumulation and p21 induction in response to doxorubicin treatment (Appendix Fig S5F). Conversely, ectopic expression of MARCH7 led to a decreased p53 response to doxorubicin treatment, as evidenced by a slower p53 accumulation and a weaker induction of p21 in MARCH7 over-expressing U2OS cells (Appendix Fig S5G), indicating that MARCH7 indeed regulates the DNA damage-induced p53 response. It has been shown that Mdm2 degradation is stimulated at the early stage of DNA damage, which contributes to the rapid induction of p53 [47]. We therefore wondered whether MARCH7 could regulate DNA damage-induced destabilization of Mdm2. The results showed that the decreased expression of Mdm2 upon doxorubicin treatment was not affected by either knockdown or ectopic expression of MARCH7 (Appendix Fig S5F and G), indicating that MARCH7 does not contribute to DNA damage-induced destabilization of Mdm2. In addition, the MARCH7–Mdm2 interaction was not affected by DNA damage (Appendix Fig S5H). Together with our findings that MARCH7 is able to stabilize Mdm2 (Fig 3), these data suggest that MARCH7 controls the p53 response to DNA damage via regulating the basal levels of Mdm2.

To examine the effect of MARCH7 on p53-mediated apoptosis, we first treated HCT116 cells with doxorubicin. As was expected, p53 knockdown almost completely inhibited doxorubicin-induced apoptosis (Appendix Fig S6A and B). Knockdown of MARCH7 dramatically increased the sensitivity of HCT116 cells to doxorubicin-induced apoptosis, however, which was reversed by simultaneous p53 knockdown (Appendix Fig S6A and B). Similar results were also obtained in U2OS cells (Appendix Fig S6C and D). In addition, MARCH7 knockdown

Figure 6. The MARCH7–Mdm2–p53 axis regulates cell proliferation, DNA damage-induced apoptosis, and tumorigenesis.

A   U2OS cells were infected with lentiviruses expressing control shRNA, MARCH7 shRNA, p53 shRNA, or both MARCH7 shRNA and p53 shRNA. Forty-eight hours after infection, cells were plated (day 1), and cell numbers were counted at the indicated time points. The shown data are mean ± SD of three independent experiments.

B   HCT116 $p53^{+/+}$ and HCT116 $p53^{-/-}$ cells were infected with lentiviruses expressing either control shRNA or MARCH7 shRNA. Forty-eight hours after infection, cells were plated (day 1), and cell numbers were counted at the indicated time points. The shown data are mean ± SD of three independent experiments.

C   MEF cells were infected with lentiviruses expressing control shRNA, MARCH7 shRNA (#4 or #5), p53 shRNA, or both MARCH7 shRNA and p53 shRNA as indicated. Forty-eight hours after infection, cells were plated (day 1), and cell numbers were counted at the indicated time points. The shown data are mean ± SD of three independent experiments.

D   HCT116 $p53^{+/+}$ and HCT116 $p53^{-/-}$ cells expressing either control shRNA or MARCH7 shRNA were treated with doxorubicin (Dox, 0.5 μg/ml) for the indicated periods of time. The nuclei were stained with Hoechst 33342. For each condition, at least 200 cells were counted, and apoptotic cells were determined by the presence of nuclear fragmentation. The shown data are mean ± SD of three independent experiments. Cell lysates were also subjected to Western blot analysis with the indicated antibodies.

E–G HCT116 cells expressing the indicated shRNAs were assayed for their ability to form colonies in soft agar. For the colony formation assay, 5×10^3 cells were used. After incubation at 37°C for 2 weeks, cells were stained with trypan blue. (E) The shown images are representative of three independent experiments. Bars: 200 μm. (F) The colonies were scored under microscope. The colony number of the cells expressing control shRNA was arbitrarily set as 1. Statistical analysis was carried out using Microsoft Excel software and GraphPad Prism to assess differences between experimental groups. Statistical significance was analyzed by Student's *t*-test and expressed as a *P*-value. The shown data are mean ± SD of three independent experiments. *** indicates $P < 0.001$. (G) Lysates from HCT116 cells used for the colony formation assay were also subjected to Western blot analysis with the indicated antibodies.

H–K 5×10^6 HCT116 cells expressing control shRNA, MARCH7 shRNA, p53 shRNA, or both MARCH7 shRNA and p53 shRNA were individually injected to the left flank and right flank of nude mice as indicated. Left and right indicate that, respectively, cells were injected into the left and right flanks of the indicated mice. Four weeks after injection, the mice were sacrificed and photographed (H). The xenografts excised from four mice in each group were compared (n = 4) (I). Tumor weights are also shown (J). The excised xenografts were homogenized for protein extraction. Protein extracts were analyzed by Western blotting with the indicated antibodies (K).

dramatically sensitized HCT116 $p53^{+/+}$ cells, but not HCT116 $p53^{-/-}$ cells, to doxorubicin-induced apoptosis (Fig 6D, Appendix Fig S6E). Furthermore, the effect of MARCH7 on p53-mediated apoptosis also occurred in normal MEF cells (Appendix Fig S6F and G). Together, these data suggest that MARCH7 plays an important role in the regulation of p53-mediated apoptosis.
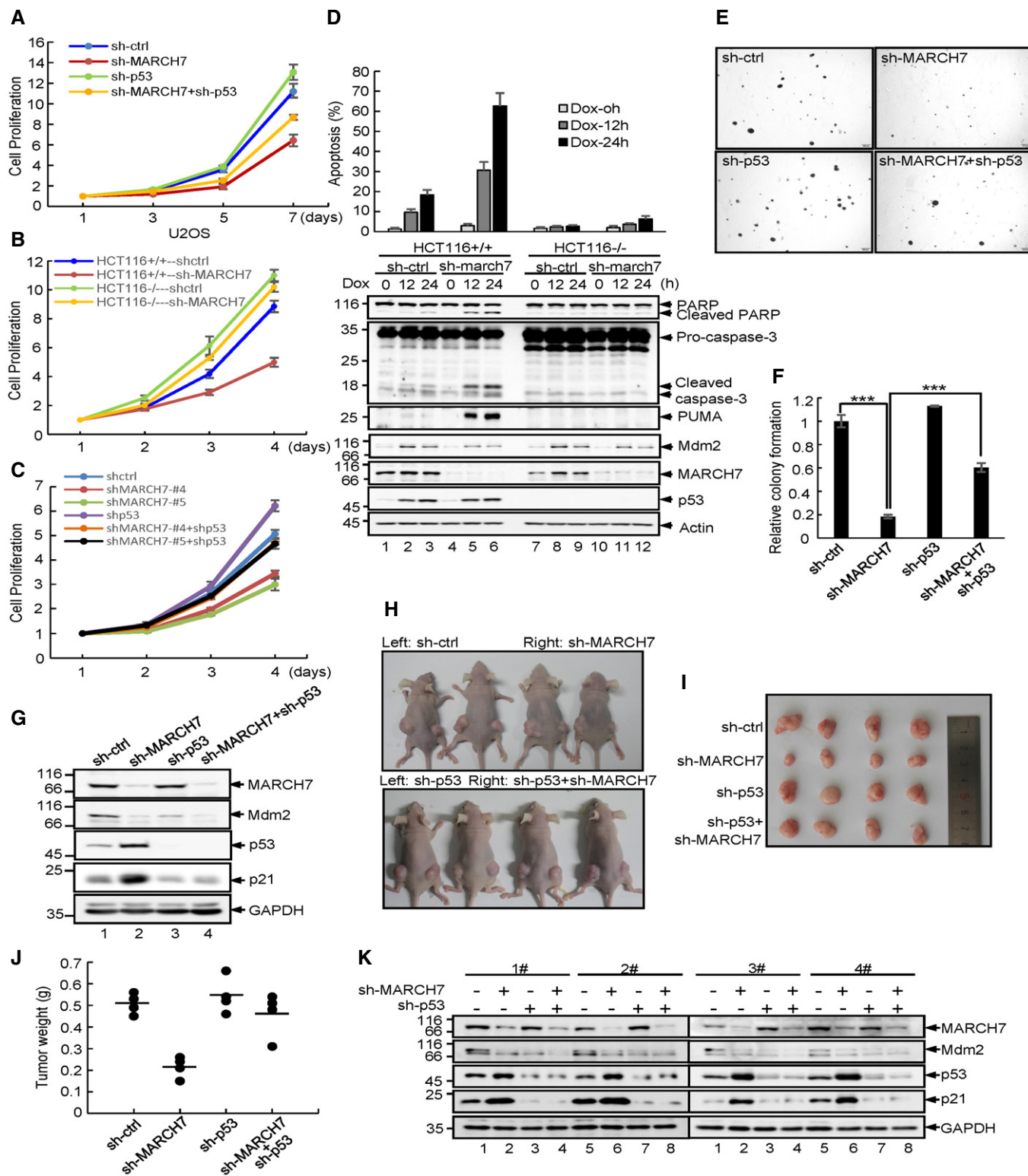

Figure 6.

To investigate the effect of MARCH7 on tumorigenicity of cells, we performed a soft agar assay. When MARCH7 was knocked down in HCT116 cells, the number of colony-forming cells was reduced by around 80% compared with the control cells (Fig 6E–G). The colony-forming ability of MARCH7 knockdown cells was greatly recovered by the simultaneous knockdown of p53 (Fig 6E–G). We next used a xenograft mouse model to determine the biological relevance of the MARCH7–Mdm2–p53 axis in cancer development. MARCH7 knockdown greatly suppressed tumorigenicity of HCT116 cells (Fig 6H–K), which was accompanied by the decreased levels of Mdm2 and the increased levels of p53 (Fig 6K). However, knockdown of MARCH7 had no obvious effect on tumorigenicity of p53-knockdown HCT116 cells (Fig 6H–K), indicating that the MARCH7–Mdm2–p53 axis indeed plays a role in the regulation of tumorigenesis. Taken together, these results suggest that MARCH7 regulates cell proliferation, DNA damage-induced apoptosis, and tumorigenesis in a p53-dependent manner.

Discussion

Mdm2 is the principle p53 antagonist that keeps p53 at low levels in unstressed cells to permit survival and growth. Therefore, investigation of mechanisms underlying the tight regulation of Mdm2 is of great importance to the understanding of p53 biology. The current work reveals that MARCH7, a RING domain-containing E3 ligase, is essential for the maintenance of Mdm2 stability. MARCH7 enhances Mdm2-dependent p53 polyubiquitination and degradation and regulates cell proliferation, DNA damage-induced apoptosis, and tumorigenesis via the inhibition of p53.

Given the importance of Mdm2 in restraining p53 activity, it is not surprising that Mdm2 is subjected to the intricate regulation by various cellular factors. It has long been recognized that autoubiquitination regulates Mdm2 abundance in cells, while recent studies suggest that the cis-E3 ligase activity of Mdm2 may not be fully responsible for its short-lived nature [48,49]. Several ubiquitin E3 ligases, such as PCAF, $SCF^{\beta-TRCP}$, XIAP, TRIM13, and NAT10, have been reported to be involved in the rapid degradation of Mdm2 [24–28]. Unlike these ubiquitin E3 ligases with Mdm2-destabilizing function, MARCH7 is able to stabilize Mdm2. MARCH7 exerts its ubiquitin E3 ligase activity to catalyze Lys^{63}-linked polyubiquitination of Mdm2, which inhibits Mdm2 autoubiquitination and degradation, thereby leading to Mdm2 stabilization. These findings uncover a novel, unexpected molecular mechanism that controls Mdm2 stability and indicate the complexity of the regulation of Mdm2. Together with the recent finding that the ubiquitin E3 ligase NEDD4-1 increases Mdm2 stability via promoting its Lys^{63}-linked polyubiquitination [50], our data suggest that Lys^{63}-linked polyubiquitination may represent an important mechanism for controlling Mdm2 stability.

In addition to above-mentioned ubiquitin E3 ligases, several deubiquitinating enzymes are also involved in the regulation of Mdm2 stability. For example, the deubiquitinating enzyme HAUSP is able to stabilize Mdm2 via removing its polyubiquitin chains [29,30]. In this study, we show that MARCH7 directly interacts and stabilizes Mdm2. Interestingly, MARCH7 levels are also subjected to the regulation by HAUSP [42]. Together, these findings indicate that MARCH7 may form a regulatory loop with HAUSP to control the stability of Mdm2.

Given the ability of MARCH7 to stabilize Mdm2, it is not surprising that MARCH7 is able to regulate Mdm2-mediated polyubiquitination and degradation of p53. As a functional consequence, MARCH7 is able to regulate both cell proliferation and DNA damage-induced apoptosis in a p53-dependent manner. It has been shown that Mdm2 undergoes accelerated degradation at early stage of DNA damage, thereby triggering the rapid p53 stabilization and activation [47]. Although MARCH7 appears not to contribute to DNA damage-induced destabilization of Mdm2, MARCH7 is capable of regulating the p53 response to DNA damage. These findings demonstrate an important function of MARCH7 in the regulation of the MDM2–p53 pathway. A recent study indicated that MARCH7 is overexpressed in ovarian cancer, where MARCH7 positively regulates both NF-kB and Wnt/β-catenin pathways [44]. By using a xenograft mouse model, we show that MARCH7 is able to regulate the tumorigenicity of HCT116 cells in a p53-dependent manner. Although a relatively small sample size ($n = 4$) was used in this study, the results nevertheless indicate the importance of the MARCH7–Mdm2–p53 axis in the regulation of tumorigenesis. Taken together, these findings imply that MARCH7 may promote tumorigenesis of different types of cancer via multiple molecular mechanisms. We should mention that p53 knockdown could not completely reverse the effect of MARCH7 on cell proliferation and DNA damage-induced apoptosis, which could be explained by two possibilities. First, although the p53 knockdown efficiency appears good based on our Western blot analysis, p53 knockdown cells may still have a small amount of residual p53. Since Mdm2 has been shown to facilitate tumorigenesis though both p53-dependent and p53-independent mechanisms [51], the second possibility is that there is the potential existence of p53-independent activity of MARCH7.

It has been reported that MARCH7 KO mice are viable and fertile. The only easily distinguishable defects are agenesis of the corpus callosum and early axonal degeneration of dorsal root ganglia. Although the MARCH7 KO mice have a normal lymphoid profile, the MARCH7-null T cells undergo hyper-proliferation after stimulation with concanavalin A [41]. In this study, we show that the effect of MARCH7 on p53 is functional in normal cells, as evidenced by the findings that MARCH7 regulates p53-dependent cell proliferation and apoptosis in MEF cells. Therefore, it would be interesting to investigate whether or not the MARCH7–Mdm2–p53 axis plays a role in mouse development in the future.

The observation that p53 is controlled largely by its master regulator Mdm2 makes the inhibition of Mdm2-mediated p53 degradation an attractive approach for re-activating p53 in p53 wild-type tumors. Nutlin-3, a small compound that blocks the Mdm2–p53 interaction, has shown promise in animal studies [52]. Several Nutlin-3 analogues such as RG7112 and RG7388 are currently in clinical trials for treatment of human cancer [53,54]. In addition, inhibition of HAUSP, a critical Mdm2-stabilizing deubiquitinating enzyme, by its specific inhibitors has shown promise in pre-clinical studies in cancers with the intact Mdm2–p53 pathway [55]. These studies have strengthened the concept that selective and non-genotoxic p53 activation by either direct or indirect Mdm2 inhibition might represent an alternative to the current cytotoxic chemotherapy. Given the important role of MARCH7 in regulating the Mdm2–p53 pathway, it may be a potential target for cancer therapy.

Materials and Methods

Reagents and antibodies

The following reagents used in this study were purchased from the indicated sources: MG132 (Calbiochem, 20 μM), cyclohex-imide (Sigma, 20 μg/ml), doxorubicin (Sigma, 0.5 μg/ml), Nutlin-3 (Sigma, 10 μM), Hoechst 33342 (Sigma, 1 μg/ml), lipofectamine 2000 (Invitrogen), complete EDTA-free protease inhibitor cocktail (Roche Applied Science), Seaplaque low melting temperature agarose (Lonza), Ni-NTA agarose beads (Qiagen), glutathione beads (GE Healthcare), antibodies against GAPDH (Santa Cruz, sc-166545, 1:5,000), GFP for immunoprecipitation (BD Biosciences, #566040), GFP for Western blotting (Santa Cruz, sc-9996, 1:1,000), MARCH7 (Santa Cruz, sc-49275, 1:200), Mdm2 (Santa Cruz, sc-965, 1:200), human p53 (Santa Cruz, sc-126, 1:1,000), mouse p53 (Abclonal, #A5804, 1:1,000), p21 (Sigma, #P1484, 1:2,000), Flag (Sigma, #F3165, 1:4,000), HA (Sigma, #H9658, 1:4,000), ubiquitin (Cell Signaling, #3936, 1:1,000), K63-linkage specific polyubiquitin (Cell Signaling, #5621, 1:1,000), HRP-conjugated secondary antibodies against mouse (sc-2005), rabbit (sc-2004), or goat IgG (sc-2768) (Santa Cruz, 1:10,000). Flag-Ubiquitin, E1, UbcH5a, and Mg^{2+}-ATP were purchased from Sigma.

Cell culture

HCT116, U2OS, MEF, $p53^{-/-}Mdm2^{-/-}$ MEF, HEK293T cell lines were cultured in Dulbecco's modified Eagle's medium (GIBCO) supplemented with 10% FBS and antibiotics (GIBCO). All cell lines were routinely tested for mycoplasma contamination before they were used for experiments.

Identification of MARCH7 as an Mdm2-interacting protein

HCT116 cells were cross-linked with 0.2% formaldehyde. The cross-linking reaction was quenched with 0.15 M of glycine (pH 7.4). Cells were lysed in RIPA buffer (50 mM Tris–HCl, pH 7.5, 150 mM NaCl, 1 mM EDTA, 0.5% Triton X-100, 0.5% NP-40, 1% sodium deoxycholates, 0.1% SDS, and 20 μM MG132) supplemented with 1× protease inhibitor cocktail. After sonication, cell lysates were pre-cleared with protein A/G-coupled agarose beads. Lysates were then immunoprecipitated with anti-Mdm2 antibody for 8 h at 4°C. After beads were extensively washed with RIPA buffer, the beads-bound proteins were eluted using elution buffer (10 mM Tris, pH 7.5, 100 mM NaCl, 2.5 mM $MgCl_2$, and 0.4% SDS) at room temperature for 30 min and analyzed by mass spectrometry. The mass spectrometry data were provided as Dataset EV1.

Real-time RT–PCR

Total RNA was isolated using Trizol (Invitrogen). 1 μg of RNA was used to synthesize cDNA using PrimeScriptTM RT reagent kit (Takara, DRR037A) according to the manufacturer's instruction. Real-time PCR was performed using SYBR premix EX Taq (TaKaRa) and analyzed with the StepOnePlus real-time PCR system (Thermo Fisher Scientific). Real-time primer sequences are shown in Appendix Table S1.

Western blot analysis and co-immunoprecipitation

Western blot analysis and co-immunoprecipitation were performed as we previously described [56]. Briefly, cells were harvested, boiled in 1× SDS loading buffer, and resolved on SDS–PAGE. For co-immuno-precipitation, cells were treated with MG132 for 6 h, before they were lysed in IP lysis buffer (50 mM Tris–HCl, pH 7.4, 150 mM NaCl, 1.5 mM $MgCl_2$, 1 mM EDTA, 0.5% NP-40, 0.5% Triton X-100, 10% glycerol, and 20 μM MG132) supplemented with 1× protease inhibitor cocktail by gentle sonication. Cell lysates were pre-cleared with protein A/G-coupled Sepharose beads for 2 h before they were immunoprecipitated with the indicated antibodies. The immunoprecipitates and input were then subjected to Western blot analysis.

RNA interference

RNA interference was performed as we previously described [57]. To generate lentiviruses expressing the indicated shRNAs, HEK293T cells grown on a 6-cm dish were transfected with 2 μg of shRNA (cloned in PLKO.1) or control vector, 2 μg of pREV, 2 μg of pGag/Pol/PRE, and 1 μg of pVSVG. Twelve hours after transfection, cells were cultured with DMEM containing 20% FBS for an additional 24 h. The culture medium containing lentivirus particles was filtered through a 0.45-μm PVDF filter (Millipore) and incubated with U2OS or HCT116 cells supplemented with 8 μg/ml polybrene (Sigma) for 24 h, followed by selection with 2 μg/ml puromycin for another 24 h. The knockdown efficiency was evaluated by Western blot analysis. The shRNA target sequences used in this study are as follows: sh-control, CCTAAGGTTAAGTCGCCCTCG; sh-MARCH7 (human), CGGAGACCATAACAGGACATT; sh-MARCH7-#2 (human), GGAAGAGATGAATCTTCAAGG; sh-MARCH7-#3 (human), GCCTTC AAGAGATCCAGAAAG; sh-MARCH7-#4 (mouse), GCAACTTAACCT GGAGGATTT; sh-MARCH7-#5 (mouse) CGAGAATCTTCTGACAAT GAA, sh-p53 (human), GACTCCAGTGGTAATCTAC; sh-p53 (mouse), CCGACCTATCCTTACCATCAT.

Protein expression and purification

The DNA sequence encoding either wild-type Mdm2 or Mdm2 C464A mutant was cloned into the pGEX-6P-1 vector, which contains a PreScission protease cleavage site. The constructs were transformed into *E. coli* Rosetta2 (DE3) cells. The cells were cultured at 37°C until the A600 nm reached 0.6 and were then induced with 0.2 mM isopropyl β-D-thiogalactoside (Promega) for 16 h at 20°C. The cells were suspended in 50 mM Tris–HCl (pH 8.0) containing 50 mM NaCl, 1 mM DTT (Promega), and 1 mg/ml lyso-zyme, incubated on ice for 30 min, and sonicated. After spinning at 13,000 *g* for 15 min at 4°C, the supernatant was incubated with glutathione Sepharose beads for 2 h. After extensive washing, the beads-bound GST fusion proteins were incubated with PreScission protease to obtain GST tag-free wild-type Mdm2 or Mdm2 C464A mutant proteins.

To over-express Flag-MARCH7 proteins, Flag-MARCH7 expressing construct was transfected into HEK293T cells. Cell lysates were immunoprecipitated with anti-Flag M2 affinity beads (Sigma). To remove the non-specific binding proteins, the beads were subjected to sequential washes with lysis buffer containing 0.25, 0.5, and 1 M

KCl as previously described [58]. The beads-bound Flag-MARCH7 proteins were eluted with 3× Flag peptide (Sigma).

In vivo ubiquitination assay

HEK293T cells were transfected with the indicated plasmids. Twenty-four hours later, cells were treated with 20 μM MG132 for an additional 6 h. The *in vivo* ubiquitination assay was then performed according to the procedure we described previously [59]. Briefly, cells were lysed in RIPA buffer (50 mM Tris–HCl, pH 7.5, 150 mM NaCl, 1 mM EDTA, 0.5% Triton X-100, 0.5% NP-40, 1% sodium deoxycholates, 0.1% SDS, and 20 μM MG132) supplemented with 1× protease inhibitor cocktail. Cell lysates were incubated with anti-Flag M2 affinity beads at 4°C for 4 h. The immunoprecipitates and input were then subjected to Western blot analysis to examine Mdm2 ubiquitination. Alternatively, cells were lysed in denaturing buffer (6 M guanidine–HCl, 0.1 M Na_2HPO_4/NaH_2PO_4, 10 mM imidazole, pH 8.0). Cell lysates were incubated with Ni-NTA agarose beads to pull down proteins conjugated to His-ubiquitin. Beads-bound proteins were then analyzed by Western blotting with anti-Mdm2 antibody.

In vitro ubiquitination assay

The *in vitro* ubiquitination assay was performed as we previously described [26]. Briefly, the purified recombinant wild-type Mdm2 or Mdm2 C464A mutant proteins were incubated with E1 (50 nM), E2 (UbcH5a, 500 nM), Flag-ubiquitin (200 μM), and either Flag-MARCH7 or Flag-MARCH7 W589A/I556A mutant proteins in 20 μl of *in vitro* ubiquitination reaction buffer (40 mM Tris–HCl, pH 7.6, 2.5 mM Mg^{2+}-ATP, and 1 mM DTT). For wild-type Mdm2 and Mdm2 C464A mutants, the reaction mixtures were incubated at 30°C for 1 h and 2 h, respectively. The reaction mixtures were analyzed by Western blotting with anti-Mdm2 antibody.

Luciferase reporter assay

To determine the effect of MARCH7 on activities of pGL3-p21 and pGL3-Noxa luciferase reporter constructs, U2OS cells expressing either control shRNA or MARCH7 shRNA were transfected with pGL3 control vector, pGL3-p21-luc, or pGL3-Noxa-luc together with Renilla luciferase plasmid. Twenty-four hours after transfection, the reporter activity was measured by using a luciferase assay kit (Promega) and plotted after normalizing with respect to Renilla luciferase activity. The data are represented as mean ± SD of three independent experiments.

Colony formation in soft agar

HCT116 cells expressing control shRNA, MARCH7 shRNA, p53 shRNA, or both MARCH7 shRNA and p53 shRNA were suspended in DMEM containing 10% FBS and 0.3% Seaplaque low melting temperature agarose (Lonza), and 1.5 ml agarose containing 5×10^3 cells was plated in one well of 6-well plates over a 1.5-ml layer of DMEM/10% FBS/0.6% agarose. Cells were incubated at 37°C for 2 weeks, before they were fixed and stained with trypan blue. The colonies were then scored under microscope.

Xenograft mouse model

5×10^6 HCT116 cells expressing control shRNA, MARCH7 shRNA, p53 shRNA, or both MARCH7 shRNA and p53 shRNA were individually injected into the dorsal flanks of 4-week-old male athymic nude mice (Shanghai SLAC Laboratory Animal Co. Ltd.) (*n* = 4 per group). Mice were used in the experiment at random. Four weeks after injection, the mice were sacrificed and tumors were excised and weighed. During testing the tumors' weight, the experimentalists were blinded to the information of tumor tissues. The excised tumors were homogenized, and proteins were extracted for Western blot analysis. Studies on animals were conducted with approval from the Animal Research Ethics Committee of the University of Science and Technology of China.

Reproducibility

All the data were repeated at least three times. The Western blot images were representative of three independent experiments.

Statistical analysis

Statistical analysis was carried out using Microsoft Excel software and GraphPad Prism to assess differences between experimental groups. Statistical significance was analyzed by Student's *t*-test and expressed as a *P*-value. *P*-values lower than 0.05 were considered to be statistically significant. One asterisk, two asterisks, and three asterisks indicate $P < 0.05$, $P < 0.01$, and $P < 0.001$, respectively.

Data availability

The mass spectrometry data from this publication are available in Dataset EV1.

Expanded View for this article is available online.

Author contributions

KZ and YM conceived and designed the project. KZ, YY, GZ, CW, and DW performed all the experiments and analyzed the data. MW provided the reagents. YM wrote the manuscript with the help of KZ All authors discussed the results and commented on the manuscript.

Conflict of interest

The authors declare that they have no conflict of interest.

References

1. Vogelstein B, Lane D, Levine AJ (2000) Surfing the p53 network. *Nature* 408: 307 – 310

2. Vousden KH, Lane DP (2007) p53 in health and disease. *Nat Rev Mol Cell Biol* 8: 275–283

3. Vousden KH, Prives C (2009) Blinded by the light: the growing complexity of p53. *Cell* 137: 413–431

4. Wasylishen AR, Lozano G (2016) Attenuating the p53 pathway in human cancers: many means to the same end. *Cold Spring Harb Perspect Med* 6: pii: a026211

5. Hussain SP, Harris CC (1999) p53 mutation spectrum and load: the generation of hypotheses linking the exposure of endogenous or exogenous carcinogens to human cancer. *Mutat Res* 428: 23–32

6. Humpton TJ, Vousden KH (2016) Regulation of cellular metabolism and hypoxia by p53. *Cold Spring Harb Perspect Med* 6: pii: a026146

7. Liu J, Zhang C, Hu W, Feng Z (2015) Tumor suppressor p53 and its mutants in cancer metabolism. *Cancer Lett* 356: 197–203

8. Tasdemir E, Maiuri MC, Galluzzi L, Vitale I, Djavaheri-Mergny M, D'Amelio M, Criollo A, Morselli E, Zhu C, Harper F *et al* (2008) Regulation of autophagy by cytoplasmic p53. *Nat Cell Biol* 10: 676–687

9. White E (2016) Autophagy and p53. *Cold Spring Harb Perspect Med* 6: a026120

10. Jiang L, Kon N, Li T, Wang SJ, Su T, Hibshoosh H, Baer R, Gu W (2015) Ferroptosis as a p53-mediated activity during tumour suppression. *Nature* 520: 57–62

11. Haupt Y, Maya R, Kazaz A, Oren M (1997) Mdm2 promotes the rapid degradation of p53. *Nature* 387: 296–299

12. Kubbutat MH, Jones SN, Vousden KH (1997) Regulation of p53 stability by Mdm2. *Nature* 387: 299–303

13. Michael D, Oren M (2003) The p53-Mdm2 module and the ubiquitin system. *Semin Cancer Biol* 13: 49–58

14. Jones SN, Roe AE, Donehower LA, Bradley A (1995) Rescue of embryonic lethality in Mdm2-deficient mice by absence of p53. *Nature* 378: 206–208

15. Montes de Oca Luna R, Wagner DS, Lozano G (1995) Rescue of early embryonic lethality in mdm2-deficient mice by deletion of p53. *Nature* 378: 203–206

16. Honda R, Yasuda H (2000) Activity of MDM2, a ubiquitin ligase, toward p53 or itself is dependent on the RING finger domain of the ligase. *Oncogene* 19: 1473–1476

17. Fang S, Jensen JP, Ludwig RL, Vousden KH, Weissman AM (2000) Mdm2 is a RING finger-dependent ubiquitin protein ligase for itself and p53. *J Biol Chem* 275: 8945–8951

18. Horn HF, Vousden KH (2007) Coping with stress: multiple ways to activate p53. *Oncogene* 26: 1306–1316

19. Momand J, Jung D, Wilczynski S, Niland J (1998) The MDM2 gene amplification database. *Nucleic Acids Res* 26: 3453–3459

20. Forslund A, Zeng Z, Qin LX, Rosenberg S, Ndubuisi M, Pincas H, Gerald W, Notterman DA, Barany F, Paty PB (2008) MDM2 gene amplification is correlated to tumor progression but not to the presence of SNP309 or TP53 mutational status in primary colorectal cancers. *Mol Cancer Res* 6: 205–211

21. Shibagaki I, Tanaka H, Shimada Y, Wagata T, Ikenaga M, Imamura M, Ishizaki K (1995) p53 mutation, murine double minute 2 amplification, and human papillomavirus infection are frequently involved but not associated with each other in esophageal squamous cell carcinoma. *Clin Cancer Res* 1: 769–773

22. Zhou M, Yeager AM, Smith SD, Findley HW (1995) Overexpression of the MDM2 gene by childhood acute lymphoblastic leukemia cells expressing the wild-type p53 gene. *Blood* 85: 1608–1614

23. Marks DI, Kurz BW, Link MP, Ng E, Shuster JJ, Lauer SJ, Brodsky I, Haines DS (1996) High incidence of potential p53 inactivation in poor outcome childhood acute lymphoblastic leukemia at diagnosis. *Blood* 87: 1155–1161

24. Linares LK, Kiernan R, Triboulet R, Chable-Bessia C, Latreille D, Cuvier O, Lacroix M, Le Cam L, Coux O, Benkirane M (2007) Intrinsic ubiquitination activity of PCAF controls the stability of the oncoprotein Hdm2. *Nat Cell Biol* 9: 331–338

25. Inuzuka H, Tseng A, Gao D, Zhai B, Zhang Q, Shaik S, Wan L, Ang XL, Mock C, Yin H *et al* (2010) Phosphorylation by casein kinase I promotes the turnover of the Mdm2 oncoprotein via the SCF(beta-TRCP) ubiquitin ligase. *Cancer Cell* 18: 147–159

26. Huang X, Wu Z, Mei Y, Wu M (2013) XIAP inhibits autophagy via XIAP-Mdm2-p53 signalling. *EMBO J* 32: 2204–2216

27. Liu X, Tan Y, Zhang C, Zhang Y, Zhang L, Ren P, Deng H, Luo J, Ke Y, Du X (2016) NAT10 regulates p53 activation through acetylating p53 at K120 and ubiquitinating Mdm2. *EMBO Rep* 17: 349–366

28. Joo HM, Kim JY, Jeong JB, Seong KM, Nam SY, Yang KH, Kim CS, Kim HS, Jeong M, An S *et al* (2011) Ret finger protein 2 enhances ionizing radiation-induced apoptosis via degradation of AKT and MDM2. *Eur J Cell Biol* 90: 420–431

29. Li M, Brooks CL, Kon N, Gu W (2004) A dynamic role of HAUSP in the p53-Mdm2 pathway. *Mol Cell* 13: 879–886

30. Cummins JM, Rago C, Kohli M, Kinzler KW, Lengauer C, Vogelstein B (2004) Tumour suppression: disruption of HAUSP gene stabilizes p53. *Nature* 428: 1 p following 486

31. Stevenson LF, Sparks A, Allende-Vega N, Xirodimas DP, Lane DP, Saville MK (2007) The deubiquitinating enzyme USP2a regulates the p53 pathway by targeting Mdm2. *EMBO J* 26: 976–986

32. Zou Q, Jin J, Hu H, Li HS, Romano S, Xiao Y, Nakaya M, Zhou X, Cheng X, Yang P *et al* (2014) USP15 stabilizes MDM2 to mediate cancer-cell survival and inhibit antitumor T cell responses. *Nat Immunol* 15: 562–570

33. Stad R, Little NA, Xirodimas DP, Frenk R, van der Eb AJ, Lane DP, Saville MK, Jochemsen AG (2001) Mdmx stabilizes p53 and Mdm2 via two distinct mechanisms. *EMBO Rep* 2: 1029–1034

34. Stad R, Ramos YF, Little N, Grivell S, Attema J, van Der Eb AJ, Jochemsen AG (2000) Hdmx stabilizes Mdm2 and p53. *J Biol Chem* 275: 28039–28044

35. Giglio S, Mancini F, Gentiletti F, Sparaco G, Felicioni L, Barassi F, Martella C, Prodosmo A, Iacovelli S, Buttitta F *et al* (2005) Identification of an aberrantly spliced form of HDMX in human tumors: a new mechanism for HDM2 stabilization. *Cancer Res* 65: 9687–9694

36. Sharp DA, Kratowicz SA, Sank MJ, George DL (1999) Stabilization of the MDM2 oncoprotein by interaction with the structurally related MDMX protein. *J Biol Chem* 274: 38189–38196

37. de Graaf P, Little NA, Ramos YF, Meulmeester E, Letteboer SJ, Jochemsen AG (2003) Hdmx protein stability is regulated by the ubiquitin ligase activity of Mdm2. *J Biol Chem* 278: 38315–38324

38. Baker RK, Haendel MA, Swanson BJ, Shambaugh JC, Micales BK, Lyons GE (1997) *In vitro* preselection of gene-trapped embryonic stem cell clones for characterizing novel developmentally regulated genes in the mouse. *Dev Biol* 185: 201–214

39. Gao W, Thompson L, Zhou Q, Putheti P, Fahmy TM, Strom TB, Metcalfe SM (2009) Treg versus Th17 lymphocyte lineages are cross-regulated by LIF versus IL-6. *Cell Cycle* 8: 1444–1450

40. Metcalfe SM (2005) Axotrophin and leukaemia inhibitory factor (LIF) in transplantation tolerance. *Philos Trans R Soc Lond B Biol Sci* 360: 1687–1694

41. Metcalfe SM, Muthukumarana PA, Thompson HL, Haendel MA, Lyons GE (2005) Leukaemia inhibitory factor (LIF) is functionally linked to

axotrophin and both LIF and axotrophin are linked to regulatory immune tolerance. *FEBS Lett* 579: 609–614

42. Nathan JA, Sengupta S, Wood SA, Admon A, Markson G, Sanderson C, Lehner PJ (2008) The ubiquitin E3 ligase MARCH7 is differentially regulated by the deubiquitylating enzymes USP7 and USP9X. *Traffic* 9: 1130–1145

43. Yan Y, Jiang W, Liu L, Wang X, Ding C, Tian Z, Zhou R (2015) Dopamine controls systemic inflammation through inhibition of NLRP3 inflammasome. *Cell* 160: 62–73

44. Hu J, Meng Y, Yu T, Hu L, Mao M (2015) Ubiquitin E3 ligase MARCH7 promotes ovarian tumor growth. *Oncotarget* 6: 12174–12187

45. Nathan JA, Kim HT, Ting L, Gygi SP, Goldberg AL (2013) Why do cellular proteins linked to K63-polyubiquitin chains not associate with proteasomes? *EMBO J* 32: 552–565

46. Swatek KN, Komander D (2016) Ubiquitin modifications. *Cell Res* 26: 399–422

47. Stommel JM, Wahl GM (2004) Accelerated MDM2 auto-degradation induced by DNA-damage kinases is required for p53 activation. *EMBO J* 23: 1547–1556

48. Itahana K, Mao H, Jin A, Itahana Y, Clegg HV, Lindstrom MS, Bhat KP, Godfrey VL, Evan GI, Zhang Y (2007) Targeted inactivation of Mdm2 RING finger E3 ubiquitin ligase activity in the mouse reveals mechanistic insights into p53 regulation. *Cancer Cell* 12: 355–366

49. Tackmann NR, Zhang Y (2017) Mouse modelling of the MDM2/MDMX-p53 signalling axis. *J Mol Cell Biol* 9: 34–44

50. Xu C, Fan CD, Wang X (2015) Regulation of Mdm2 protein stability and the p53 response by NEDD4-1 E3 ligase. *Oncogene* 34: 281–289

51. Li Q, Lozano G (2013) Molecular pathways: targeting Mdm2 and Mdm4 in cancer therapy. *Clin Cancer Res* 19: 34–41

52. Vassilev LT, Vu BT, Graves B, Carvajal D, Podlaski F, Filipovic Z, Kong N, Kammlott U, Lukacs C, Klein C *et al* (2004) *In vivo* activation of the p53 pathway by small-molecule antagonists of MDM2. *Science* 303: 844–848

53. Burgess A, Chia KM, Haupt S, Thomas D, Haupt Y, Lim E (2016) Clinical overview of MDM2/X-targeted therapies. *Front Oncol* 6: 7

54. Zhao Y, Aguilar A, Bernard D, Wang S (2015) Small-molecule inhibitors of the MDM2-p53 protein-protein interaction (MDM2 Inhibitors) in clinical trials for cancer treatment. *J Med Chem* 58: 1038–1052

55. Tavana O, Gu W (2017) Modulation of the p53/MDM2 interplay by HAUSP inhibitors. *J Mol Cell Biol* 9: 45–52

56. Wang X, Zha M, Zhao X, Jiang P, Du W, Tam AY, Mei Y, Wu M (2013) Siva1 inhibits p53 function by acting as an ARF E3 ubiquitin ligase. *Nat Commun* 4: 1551

57. Yang F, Zhang H, Mei Y, Wu M (2014) Reciprocal regulation of HIF-1alpha and lincRNA-p21 modulates the Warburg effect. *Mol Cell* 53: 88–100

58. Tang J, Qu LK, Zhang J, Wang W, Michaelson JS, Degenhardt YY, El-Deiry WS, Yang X (2006) Critical role for Daxx in regulating Mdm2. *Nat Cell Biol* 8: 855–862

59. Gu H, Li Q, Huang S, Lu W, Cheng F, Gao P, Wang C, Miao L, Mei Y, Wu M (2015) Mitochondrial E3 ligase March5 maintains stemness of mouse ES cells via suppression of ERK signalling. *Nat Commun* 6: 7112